Cobalt-Hydride Catalyzed Alkene-Carboxylate Transposition (ACT) of Allyl Carboxylates via 1,2-Radical Migration (RaM)

Gaoyuan Zhao,*,[1] Arman Khosravi,#,[1] Sahil Sharma,#,[1] Djamaladdin G. Musaev,*,[2] Ming-Yu Ngai*,[1]

[1]Department of Chemistry, Purdue University, West Lafayette, Indiana, 47907, United States. [2]Cherry L. Emerson Center for Scientific Computation, and Department of Chemistry, Emory University, Atlanta, GA 30322, United States.

ABSTRACT: The Alkene-Carboxylate Transposition (ACT) of allyl carboxylates is one of the most atom-economic and synthetically reliable transformations in organic chemistry, as allyl carboxylates are versatile synthetic intermediates. Classic ACT transformations, including 3,3-sigmatropic rearrangement and transition metal-catalyzed allylic rearrangement, typically yield 1,2-alkene/1,3-acyloxy shifted products through a two-electron process. However, position-altered ACT to produce distinct 1,3-alkene/1,2-acyloxy shifted products has remained elusive. Here, we report the first cobalt-hydride catalyzed ACT of allyl carboxylates, enabling access to these unprecedented 1,3-alkene/1,2-acyloxy shifted products via a 1,2-radical migration (RaM) strategy. This transformation demonstrates broad functional group tolerance, is suitable for late-stage modification of complex molecules, and is amenable to gram-scale synthesis. It also expands the reaction profiles of both allyl carboxylates and cobalt catalysis. Preliminary experimental and computational studies suggest a mechanism involving metal-hydride hydrogen atom transfer (MHAT) and 1,2-RaM process. This reaction is expected to serve as the basis for the development of versatile Co-H catalyzed transformations of allyl carboxylates, generating a wide array of valuable building blocks for synthetic, medicinal, and materials chemistry.

Allyl carboxylates are essential synthetic intermediates, known for their versatility and capacity to undergo a wide range of reliable derivatizations.[1] Given their importance, harnessing the new reactivity of allyl carboxylates is crucial for advancing organic synthesis. Among the transformations available, the Alkene-Carboxylate Transposition (ACT) of allyl carboxylates stands out as one of the most atom-economical and synthetically reliable methods in organic chemistry. The classical 3,3-sigmatropic rearrangement of allyl carboxylates is widely applied in industries such as fragrances and pharmaceuticals, where it serves as a key building block for complex molecular architectures.[2] Additionally, transition metal-catalyzed allylic rearrangement, which includes ACT, further enriches the repertoire of these transformations by yielding thermodynamically stable 1,2-alkene/1,3-acyloxy shifted products through a two-electron process (Figure 1A).[3] However, the development of position-altered ACT of allyl carboxylates to produce distinct 1,3-alkene/1,2-acyloxy shifted products remains elusive.

Cobalt catalysis has become a dynamic field in organic synthesis, driven by cobalt's unique reactivity and abundance in the Earth's crust.[4] Notably, cobalt hydride species, common active catalytic intermediates, have shown remarkable efficacy in redox-neutral catalysis, particularly in olefin isomerization via β-hydride elimination/migratory insertion or metal-hydride hydrogen atom transfer (MHAT).[3a, 3d, 4d, 5] These processes generate synthetically valuable olefins, expanding the chemist's toolkit. Typically, cobalt-hydride transfers an H-atom to an olefin, creating a C-H bond at a less electronically stabilized position and forming a radical center. A subsequent H-atom abstraction at a more stabilized position results in the isomerized olefin. More recently, elegant contra-thermodynamic positional olefin isomerization has been achieved by merging cobalt catalysis with photochemical irradiation.[6] Despite these advances, Co-H catalyzed alkene isomerization accompanied by functional group migration, such as an acyloxy shift, has not been reported. Inspired by the Surzur-Tanner rearrangement—where a β-(acyloxy)alkyl radical undergoes 1,2-radical migration (RaM) via an acyloxy shift to yield a more stable radical intermediate[7]— we wonder if we could merge MHAT with 1,2-RaM to achieve position-altered ACT of allyl carboxylates, producing 1,3-alkene/1,2-acyloxy shifted products distinct from those formed by 3,3-sigmatropic rearrangement or transition metal-catalyzed alkene/carboxylate transposition. Our mechanistic hypothesis involves Co-H catalyzed MHAT to form radical intermediate **I**, followed by 1,2-radical migration (RaM) and site-selective Co-catalyzed HAT, yielding the desired products while regenerating the Co-H catalyst (Figure 1C). Successfully achieving this transformation will be significant because it (i) expands the reaction profiles of allyl carboxylates and cobalt-catalyzed redox-neutral transformations, (ii) enables the ACT of allyl carboxylates to access products distinct from conventional two-electron processes, (iii) allows new bond disconnection in organic synthesis, and (iv) establishes a general platform for 1,3-hydrofunctionalization of allyl carboxylates through the homolytic activation of C-O bonds in carboxylates.
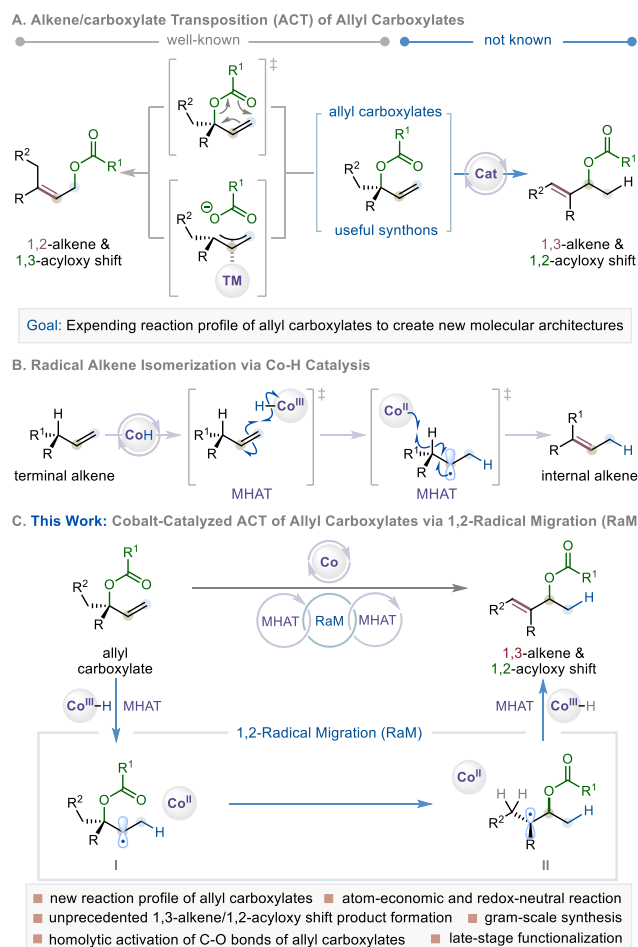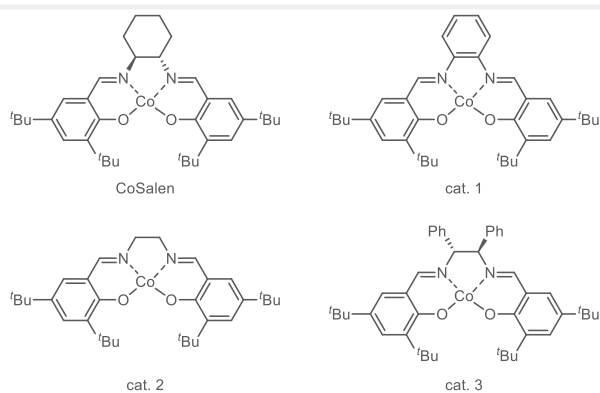
Figure 1. Reactions of allyl carboxylates and cobalt-catalyzed olefine isomerization.

To test our hypothesis, we commence our study using 4-vinyltetrahydro-2H-pyran-4-yl benzoate **1a** as the model substrate (Table 1). Through a systematic exploration of reaction parameters, we found that employing CoSalen as the catalyst (20 mol%), along with PhSiH$_3$ (0.75 equiv) and Selectfluor (0.75 equiv) in a solvent mixture of DCE/*tert*-BuOH (0.04 M, 4:1), at a reaction temperature of 90 °C for 48 hours, yielded the desired ACT product **2a** in an 87% yield (entry 1). The essential role of the cobalt catalyst in facilitating the desired reactivity was demonstrated by the complete lack of reaction in its absence (entry 2). The use of different cobalt catalysts, such as cat. 1, cat. 2, and cat. 3, lowered the yield to 43% - 52% (entry 3-5). Furthermore, Co(OAc)$_2$·4H$_2$O was ineffective, failing to produce the desired product (entry 6), indicating that the ligand scaffold significantly influences the reactivity. PhSiH$_3$ was crucial for initiating the reaction, acting as the hydrogen source to form the active Co-H species. The reaction did not proceed when PhSiH$_3$ was omitted or replaced with Et$_3$SiH or Ph$_3$SiH (entries 7-9). Additionally, the use of Selectfluor was vital for converting Co^{II} to Co^{III}-F, whereas employing NFSI as an oxidant led to decreased yields (entries 10-11).

Replacing DCE with MeCN reduced the reaction efficiency (entry 12). Consistent with many Co-H catalytic systems, the addition of a polar, protic solvent, *t*-BuOH, was crucial for maintaining high catalytic efficiency by generating an alkoxysilane in situ (entry 13).[5l, 8] Intriguingly, water also served as an effective additive, yielding a comparable amount of the desired product (entry 14). An elevated temperature of 90 °C was necessary to facilitate 1,2-radical migration, leading to a more stable radical intermediate (entry 15). Notably, the reaction is insensitive to air and afforded the desired product in comparable yield, demonstrating its robustness and operational simplicity (entries 16).
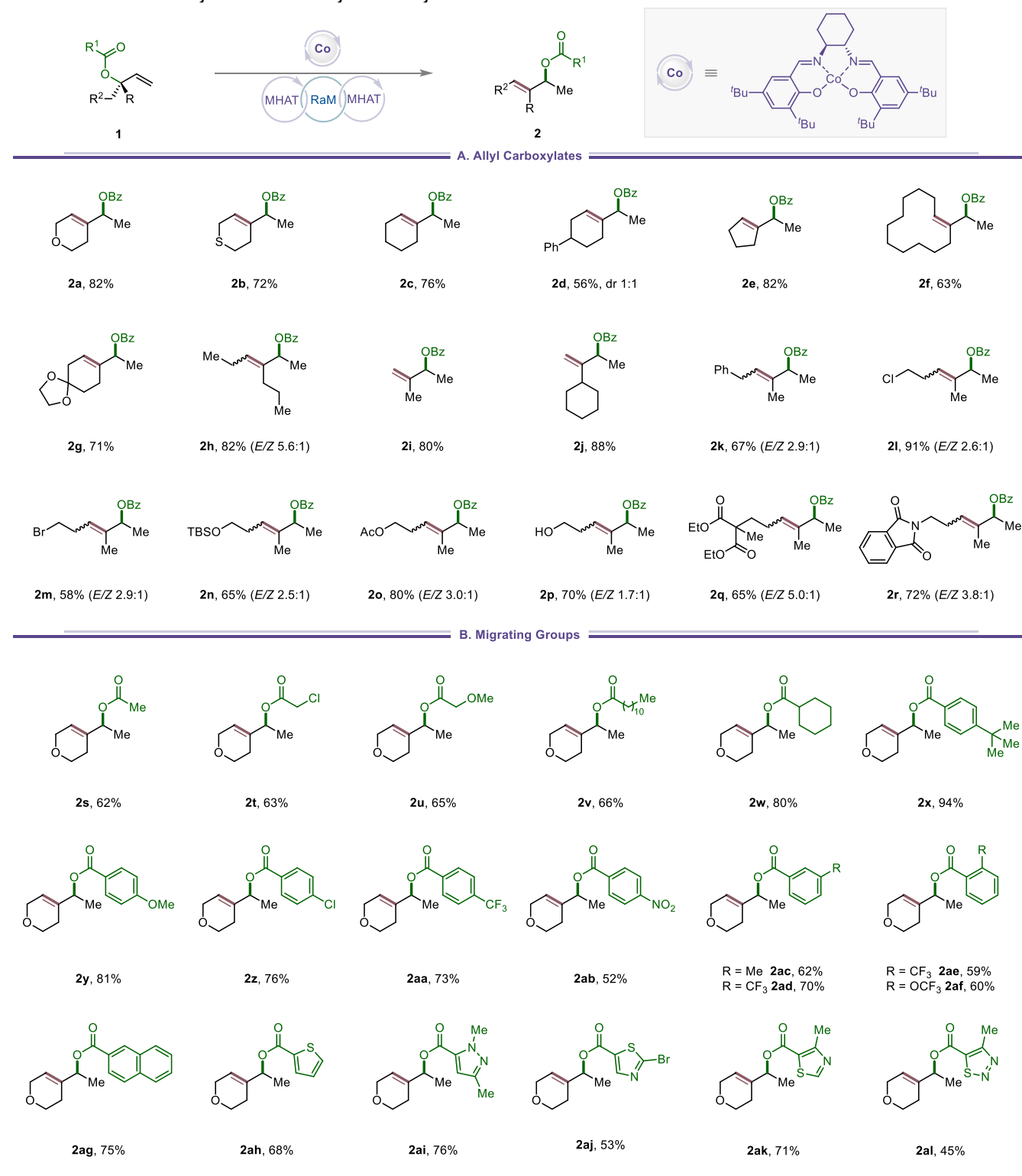
Table 1. Selected optimization experiments[a]

Entry	Deviation from the standard conditions	Yield (%)
1	none	87
2	withour CoSalen	N.R.
3	cat. 1 instead of CoSalen	52
4	cat. 2 instead of CoSalen	51
5	cat. 3 instead of CoSalen	43
6	Co(OAc)$_2$ 4H$_2$O instead of Co(trans-)Salen	0
7	without PhSiH$_3$	N.R.
8	Et$_3$SiH instead of PhSiH$_3$	N.R.
9	Ph$_3$SiH instead of PhSiH$_3$	N.R.
10	without selectfluor	64
11	NFSI instead of selectfluor	59
12	MeCN instead of DCE	31
13	Without t-BuOH	62
14	H$_2$O instead of t-BuOH	76
15	rt	36
16	Air	80

[a]See Supporting Information (SI) for experimental details. Reaction yields were determined by ^{1}H-NMR using CH$_2$Br$_2$ as an internal standard. Bz, benzoyl; DCE, 1,2-dichloroethane; N.R., no reaction.

Table 2. Cobalt-Catalyzed ACT of Allyl Carboxylates [a]

A. Allyl Carboxylates

2a, 82% **2b**, 72% **2c**, 76% **2d**, 56%, dr 1:1 **2e**, 82% **2f**, 63%

2g, 71% **2h**, 82% (*E/Z* 5.6:1) **2i**, 80% **2j**, 88% **2k**, 67% (*E/Z* 2.9:1) **2l**, 91% (*E/Z* 2.6:1)

2m, 58% (*E/Z* 2.9:1) **2n**, 65% (*E/Z* 2.5:1) **2o**, 80% (*E/Z* 3.0:1) **2p**, 70% (*E/Z* 1.7:1) **2q**, 65% (*E/Z* 5.0:1) **2r**, 72% (*E/Z* 3.8:1)

B. Migrating Groups

2s, 62% **2t**, 63% **2u**, 65% **2v**, 66% **2w**, 80% **2x**, 94%

2y, 81% **2z**, 76% **2aa**, 73% **2ab**, 52% R = Me **2ac**, 62% / R = CF$_3$ **2ad**, 70% R = CF$_3$ **2ae**, 59% / R = OCF$_3$ **2af**, 60%

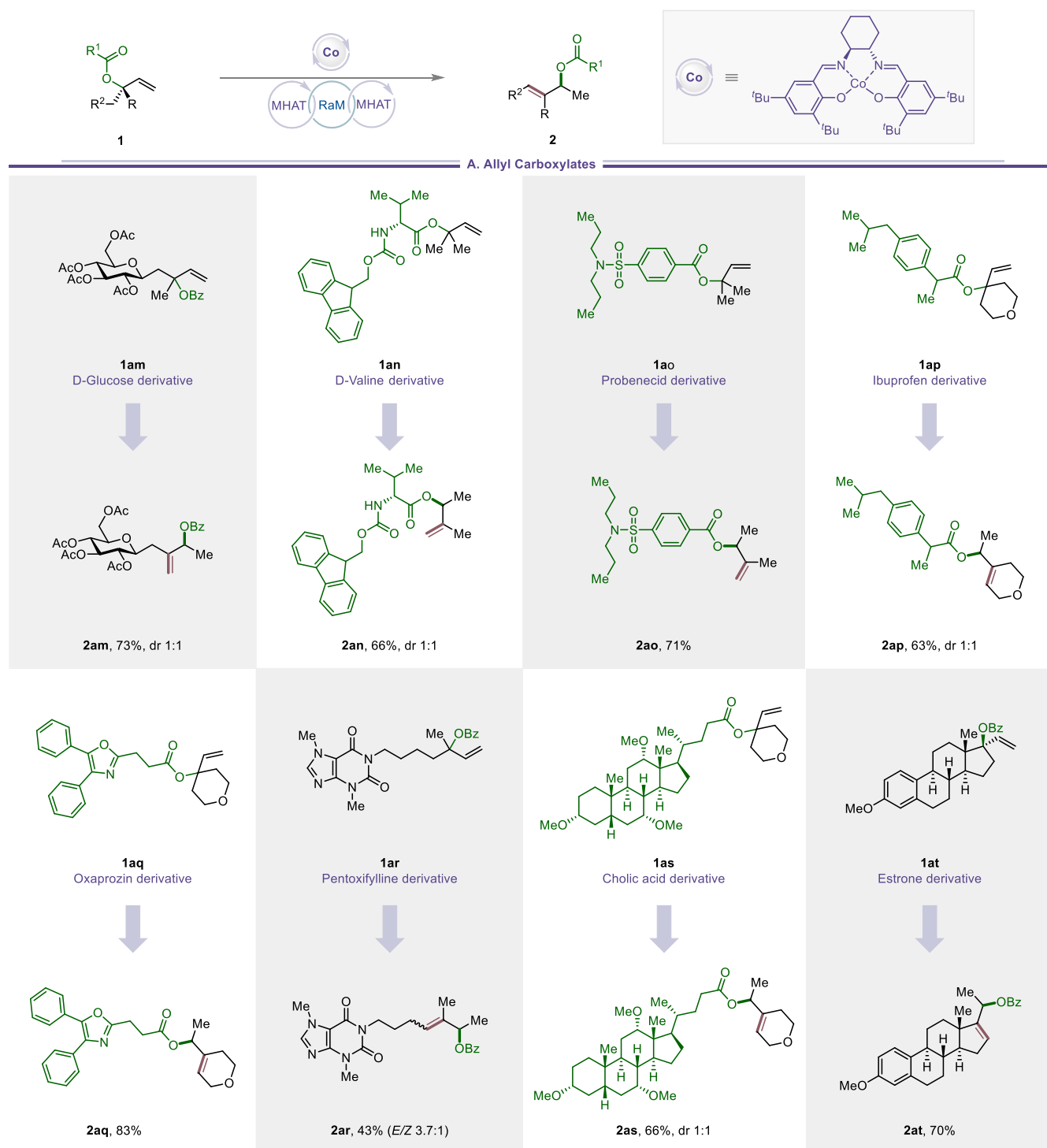**2ag**, 75% **2ah**, 68% **2ai**, 76% **2aj**, 53% **2ak**, 71% **2al**, 45%

[a]See SI for experimental details, **1** (0.200 mmol, 1.00 equiv), CoSalen (20.0 mol%), PhSiH$_3$ (0.75 equiv), selectfluor (0.75 equiv), DCE (8.00 mL), *t*-BuOH (2.00 mL), 90 °C, 48 h.

With the optimized reaction conditions in hands, we explored the reaction scope of allyl carboxylates, as summarized in Table 2. A diverse array of substituted allyl carboxylates, including both cyclic and linear frameworks, reacted smoothly, delivering the corresponding products **2a**-**2r** in satisfactory yields ranging from 56% to 91%. Substrates featuring cyclic ether and thioether moieties (**2a** & **2b**), diverse cyclic ring systems including 5, 6, and 12-membered rings (**2c**-**2f**), and those with the ethylene ketal group (**2g**) were compatible under the standard reaction

Table 3. Late-Stage Modification of Complex Molecules[a]

A. Allyl Carboxylates

1am — D-Glucose derivative → **2am**, 73%, dr 1:1

1an — D-Valine derivative → **2an**, 66%, dr 1:1

1ao — Probenecid derivative → **2ao**, 71%

1ap — Ibuprofen derivative → **2ap**, 63%, dr 1:1

1aq — Oxaprozin derivative → **2aq**, 83%

1ar — Pentoxifylline derivative → **2ar**, 43% (E/Z 3.7:1)

1as — Cholic acid derivative → **2as**, 66%, dr 1:1

1at — Estrone derivative → **2at**, 70%

[a]See SI for experimental details. **1** (0.200 mmol, 1.00 equiv), CoSalen (20.0 mol%), PhSiH$_3$ (0.75 equiv), selectfluor (0.75 equiv), DCE (8.00 mL), t-BuOH (2.00 mL), 90 °C, 48 h.

conditions. The reaction scope can be further extended to acyclic system. For example, a dimethyl-substituted allyl carboxylate reacted smoothly, forming the arranged allyl carboxylate **2i** in 80% yield. For non-symmetric allyl carboxylates, such as the methylcyclohexanyl-substituted substrate, where competition in the HAT step occurs between primary and tertiary hydrogen atoms, the Co exclusively abstracts the primary hydrogen atom, forming the kinetic, terminal alkene product **2j** in excellent yield. Conversely, when HAT competes between secondary and primary hydrogen atoms, cobalt catalyst preferentially abstracts from the secondary carbon, yielding thermodynamically more stable products **2k-2r**. These findings demonstrate that the CoSalen catalysts are highly sensitivity to substrate sterics. Moreover, a diverse array of functional groups, such as phenyl, chloro, bromo, siloxyl, acyloxyl,

hydroxyl, ester, and phthalimide, were well-tolerated, furnishing the corresponding products **2k-2r** in good to excellent yields.

Further exploration revealed a wide range of effective migrating groups under standard conditions, including acetate, 2-chloroacetate, and 2-methoxylacetate (**2s-2u**). Additionally, dodecanoate and cyclohexanecarboxylate proved to be proficient migrating groups, yielding 66% and 80% of the desired products, respectively (**2v-2w**). Notably, both electron-donating and electron-withdrawing substituents at various positions of the aromatic ring underwent ACT, affording the corresponding products (**2x-2af**) in yields ranging from 59% to 94%. The versatility of the developed protocol was further demonstrated by successful migration of allyl carboxylates featuring ortho-, meta-, and para-substituted benzoate groups. Moreover, 2-naphthanenyl carboxylates and heteroaryl carboxylates, including thiophene-2-carboxylate, 1,3-dimethyl-1H-pyrazole-5-carboxylate, 2-bromothiazole-5-carboxylate, 4-methylthiazole-5-carboxylate, and 4-methyl-1,2,3-thiadiazole-5-carboxylate, all underwent efficient migration, yielding the corresponding products (**2ag-2al**) in good yields.

The development of therapeutic medications often relies on late-stage modification of complex or bioactive molecules.[9] To demonstrate the versatility of our method, we subjected a series of natural product- and drug-conjugated substrates to standard reaction conditions. Notably, D-Glucose, D-Valine, Probenecid, Ibuprofen, Oxaprozin, and Pentoxifylline-derived allyl carboxylates reacted well, providing the desired products (**2am-2ar**) with yields ranging from 43% to 83%. Furthermore, derivatives of Cholic acid and Estrone showed good reactivity, producing products (**2as-2at**) with yields of 66% and 70%, respectively.

To demonstrate the scalability and synthetic utility of the cobalt-catalyzed ACT process, we performed a gram-scale reaction that scaled to 5 mmol, achieving a 77% yield of the desired product **2h**. Subsequent transformations illustrated the versatility of the rearranged allyl carboxylate products: hydrogenation yielded the saturated ester **3** with a 95% yield; epoxidation of the newly formed alkene was successful using *meta*-chloroperoxybenzoic acid (m-CPBA); ozonolysis produced a 2-carboxylate ketone **5** with an 81% yield, showcasing diverse synthetic pathways. Additionally, an organo-photocatalyzed hydrothiolation reaction demonstrated potential applications in ligation and material science.[10] The Tsuji-Trost reaction with diethyl malonate as the nucleophile produced allylation products **7** and **8** with a 66% yield. Finally, dibromination with bromine generated the 1,2-dibromo product 9, further demonstrating the versatility of the products.

Scheme 1. Large-Scale Reaction and Post-Functionalization[a]

A. Gram-scale Synthesis
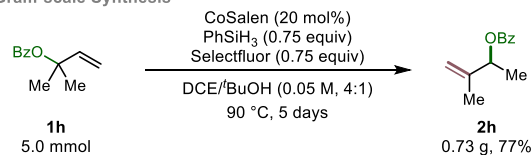
B. Post-functionalization of Product 2h
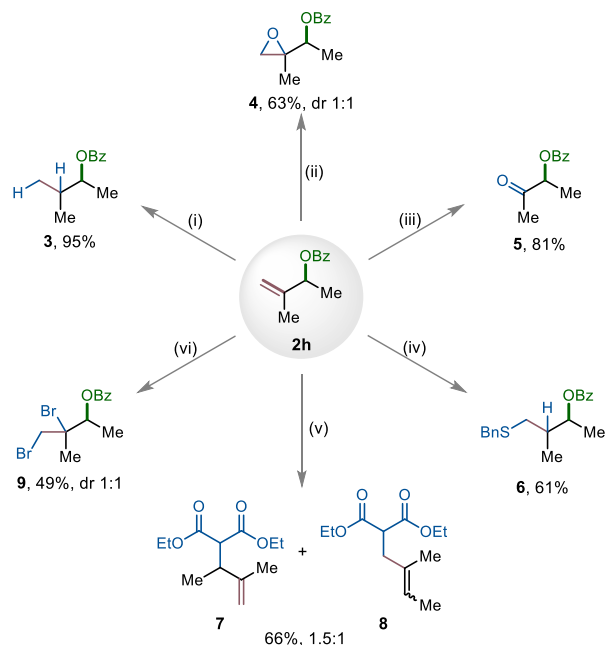
[a]See SI for experimental details. (i) Pd/C (10 wt%), H₂, MeOH (0.100 M), rt, 12h. (ii) m-CPBA (1.50 equiv), DCM (0.100 M), 0 °C – rt, 3h. (iii) O₃, PPh₃ (2.00 equiv), DCM (0.001 M), -78 °C, 10 min. (iv) BnSH (1.00 equiv), Mes-Acr-Me⁺BF₄⁻ (5.00 mol%), MeCN (0.500 M), 24 W blue LED, rt, 16h. (v) Diethyl malonate (1.50 equiv), NaH (1.50 equiv), Pd(PPh₃)₄ (1.00 mol%), THF (0.100 M), rt, 16h. (vi) Br₂ (1.50 equiv), CHCl₃ (0.100 M), 0 °C – rt, 12h.

To elucidate the mechanism of the cobalt-catalyzed ACT reaction, we conducted a series of experimental and computational studies. The introduction of a radical scavenger, 2,2,6,6-tetramethylpiperidine 1-oxyl (TEMPO), significantly inhibited the reaction (Fig. S1). A radical-clock reaction led to a ring-opening alkene product (**2au**) (Figure 2A). These radical trap and radical clock experiments suggested a radical-mediated mechanism. Crossover experiments with substrates **1h** and **1ag** resulted in exclusive formation of non-crossover products **2h** and **2ag**, indicating an intramolecular acyloxy shift mechanism (Figure 2B). Further studies using deuterated substrates revealed a deuterium-shifted product **2aw** (Figure 2C), and crossover experiments with deuterated and non-deuterated substrates produced crossover products **2a-d**, supporting an intermolecular MHAT process (Figure 2D). Kinetic isotope effect (KIE) studies showed a KIE value of 2.9, implying a primary kinetic isotope effect (Figure 2E). Additionally, ¹⁸O-labeling experiments with substrate **¹⁸O-1h** yielded products **¹⁸O-2h-1** and **¹⁸O-2h-2** in a 5.4:1 ratio, suggesting both [1,2]- and [2,3]-acyloxy group shift pathways are operational (Figure 2F).

 ORCID: https://orcid.org/0000-0002-3055-6662

A. Radical Clock Experiment:

BzO / Me Me

1au

standard conditions →

OBz / Me / Me

2au, 41% (*E/Z* 3.2:1)

■ **Implication**: The reaction likely involves a radical mechanism

B. Crossover Reaction:

1ag, 0.01 mmol

standard conditions →

2h, 72%   +   **2ag**, 87%

1h, 0.01 mmol

crossover products

BzO / Me   +   Me

2a, 0%   +   **2av**, 0%

not observed

■ **Implication**: The ester migration likely proceeds through intramolecular pathway

C. Deuterium Labelling Experiment:

BzO / D_3C CD_3

1aw

standard conditions →

(0.92 D) D / D / OBz / H/D (0.45 D) / CD_3

2aw, 59%

■ **Implication**: The reaction occurs via HAT pathway

D. Deuterium Crossover Reaction:

BzO / D_3C CD_3

1aw, 0.01 mmol

BzO / O

1a, 0.01 mmol

standard conditions →

(0.86 D) D / D / OBz / H/D (0.14 D) / CD_3

2aw, 38%

BzO / H/D (0.19 D) / O

2a, 66%

■ **Implication**: Cross-over products implies intermolecular MHAT process

E. Kinetic Isotope Effect studies:

BzO / H_3C CH_3

1h, 0.01 mmol

BzO / D_3C CD_3

1aw, 0.01 mmol

standard conditions

$P_H/P_D = 2.9:1$

→

H / OBz / Me / CH_3

2h, 44%

D / D / OBz / Me / CD_3

2aw, 15%

■ **Implication**: $P_H/P_D > 1.4$ suggests primary KIE

F. ^{18}O-Labeling Experiment:

Ph ^{18}O / O / Me Me

^{18}O-1h (95% ^{18}O)

standard conditions / 83% →

O^{18} / O / Ph / Me   + ^{18}O / O / Ph / me

^{18}O-2h-1   5.4 : 1   **^{18}O-2h-2**

■ **Implication**: 1,2-RaM likely proceeds through both [1,2]- and [2,3]-TS

G. Energy Profile of Cobalt-Catalyzed Alkene-Carboxylates Transposition (ACT) of Allyl Carboxylates:

ΔG (kcal/mol)

TS-1b 18.0

TS-1a 12.9

[1,2]-TS 3.9

[2,3]-TS 5.4

TS-2a 6.8

TS-2b 11.4

0.0 (I + 1h)

II −3.3

III −6.9

2h −4.9

2h' −7.4

MHAT — 1,2-RaM — MHAT

TS-1a   [1,2]-TS   [2,3]-TS   TS-2a
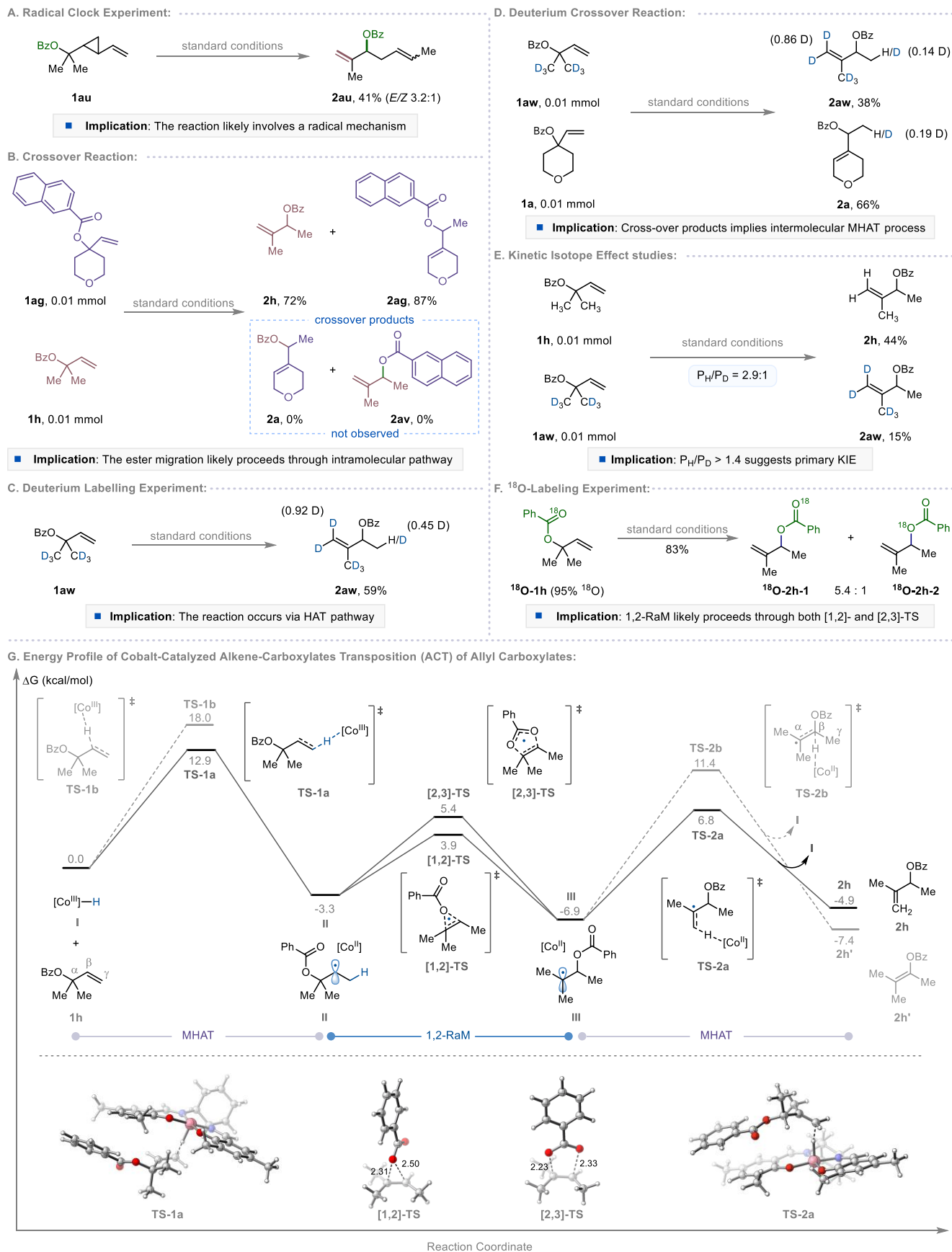
2.31 / 2.50   2.23 / 2.33

Reaction Coordinate

Figure 2. Mechanistic studies. All energies are in kcal/mol and are relative to **I** and **1h**. Distances between the critical atoms are in Å (see SI for details). The 3D representation was prepared using CYLview.[11]

Density functional theory (DFT) analysis showed that the transfer of a hydrogen atom from [Co^{III}]-H to the γ position of allyl carboxylate (**TS-1a**) is 5.10 kcal/mol more favorable than to the β position (**TS-1b**), resulting in the formation of radical intermediate **II** (Figure 2G). The transition state energy for the 1,2-RaM in the 3-membered ring (**[1,2]-TS**) is 1.5 kcal/mol lower than in the 5-membered ring (**[2,3]-TS**), indicating a preference for the [1,2] pathway, resemble with experimental selectivity (Figure 2F). Additionally, the abstraction of a hydrogen atom from radical intermediate **III** by the [Co^{II}] catalyst is the rate-determining step (**TS-2a**), with an energy barrier of 13.7 kcal/mol, consistent with the KIE studies (Figure 2E). This step is more favorable than abstracting the hydrogen atom from the β-carbon (**TS-2b**, $\Delta\Delta G^{\ddagger}$ = 11.4 kcal/mol), explaining the regioselective formation of product **2**.

Based on our mechanistic studies and literature reports,[5b-d, 12] we propose a catalytic cycle as depicted in Figure 3. The reaction begins with [Co^{II}], Selectfluor, and phenyl silane forming the active catalyst [Co^{III}]-H. This catalyst then performs HAT on allyl carboxylate **1a**, generating [Co^{II}] and the secondary radical intermediate **II**. Upon heating, intermediate **II** undergoes 1,2-RaM through both [1,2] and [2,3] transition states, forming the more stable radical intermediate **III**. Finally, HAT from intermediate **III** to [Co^{II}] produces the desired product and regenerates the [Co^{III}]-H catalyst, thus completing the catalytic cycle.
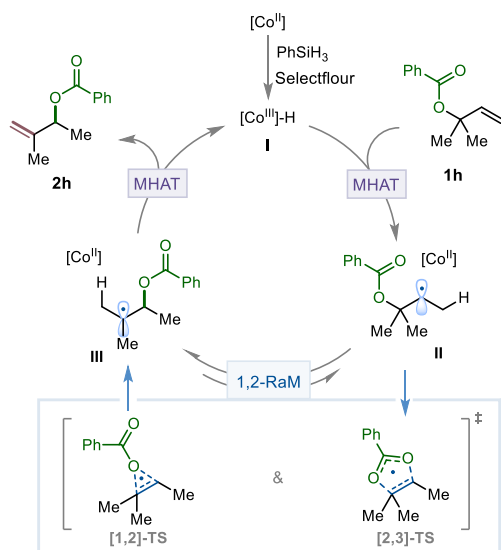

Figure 3. Proposed reaction mechanism.

In summary, we have developed a cobalt-catalyzed ACT reaction of allyl carboxylate, accessing structurally distinct 1,3-alkene/1,2-acyloxy shifted product. The reaction features a broad substrate scope, accommodating various functional groups, and enables late-stage modifications of complex molecules as well as gram-scale synthesis. Preliminary mechanistic studies suggest a radical mechanism involving 1,2-RaM and MHAT processes. We anticipate that this protocol will serve as the basis for developing various 1,3-hydrofunctionalization reactions, thereby expanding the reaction profile of allyl carboxylates.

AUTHOR INFORMATION

Corresponding Author

zhao1373@purdue.edu
dmusaev@emory.edu
mngai@purdue.edu

Notes
#These authors contributed equally and are listed in alphabetical order. The authors declare no competing financial interests.

REFERENCES

1.   (a) Weaver, J. D.; Recio III, A.; Grenning, A. J.; Tunge, J. A., Transition metal-catalyzed decarboxylative allylation and benzylation reactions. *Chem. Rev.* **2011**, *111*, 1846-1913; (b) Feng, J.; Holmes, M.; Krische, M. J., Acyclic quaternary carbon stereocenters via enantioselective transition metal catalysis. *Chem. Rev.* **2017**, *117*, 12564-12580; (c) Cheng, Q.; Tu, H.-F.; Zheng, C.; Qu, J.-P.; Helmchen, G. n.; You, S.-L., Iridium-catalyzed asymmetric allylic substitution reactions. *Chem. Rev.* **2018**, *119*, 1855-1969; (d) Kim, S. W.; Schwartz, L. A.; Zbieg, J. R.; Stivala, C. E.; Krische, M. J., Regio-and Enantioselective Iridium-Catalyzed Amination of Racemic Branched Alkyl-Substituted Allylic Acetates with Primary and Secondary Aromatic and Heteroaromatic Amines. *J. Am. Chem. Soc.* **2018**, *141*, 671-676; (e) Pamies, O.; Margalef, J.; Canellas, S.; James, J.; Judge, E.; Guiry, P. J.; Moberg, C.; Backvall, J.-E.; Pfaltz, A.; Pericas, M. A., Recent advances in enantioselective Pd-catalyzed allylic substitution: from design to applications. *Chem. Rev.* **2021**, *121*, 4373-4505.

2.   (a) Ilardi, E. A.; Stivala, C. E.; Zakarian, A., [3, 3]-Sigmatropic rearrangements: recent applications in the total synthesis of natural products. *Chem. Soc. Rev.* **2009**, *38*, 3133-3148; (b) Serra-Muns, A.; Guérinot, A.; Reymond, S.; Cossy, J., Silica gel-mediated rearrangement of allylic acetates. Application to the synthesis of 1, 3-enynes. *Chem. Commun.* **2010**, *46*, 4178-4180; (c) Sølvhøj, A.; Taarning, E.; Madsen, R., Methyl vinyl glycolate as a diverse platform molecule. *Green Chem.* **2016**, *18*, 5448-5455; (d) Nakayama, A.; Sodenaga, R.; Gangarajula, Y.; Taketoshi, A.; Murayama, T.; Honma, T.; Sakaguchi, N.; Shimada, T.; Takagi, S.; Haruta, M., Enhancement effect of strong metal-support interaction (SMSI) on the catalytic activity of substituted-hydroxyapatite supported Au clusters. *J. Catal.* **2022**, *410*, 194-205.

3.   (a) Henry, P. M., Palladium (II)-catalyzed exchange and isomerization reactions. III. Allylic esters isomerization in acetic acid catalyzed by palladium (II) chloride. *J. Am. Chem. Soc.* **1972**, *94*, 5200-5206; (b) Henry, P. M., Palladium (II)-catalyzed exchange and isomerization reactions. *Acc. Chem. Res.* **1973**, *6*, 16-

24; (c) Overman, L. E.; Knoll, F. M., Palladium (II)-catalyzed rearrangement of allylic acetates. *Tetrahedron Lett.* **1979**, *20*, 321-324; (d) Mukhopadhyay, M.; Reddy, M. M.; Maikap, G.; Iqbal, J., Cobalt (II)-catalyzed conversion of allylic alcohols/acetates to allylic amides in the presence of nitriles. *J. Org. Chem.* **1995**, *60*, 2670-2676; (e) Jessen, B. M.; Ondozabal, J. M.; Pedersen, C. M.; Sølvhøj, A.; Taarning, E.; Madsen, R., Palladium (o)‐Catalyzed Rearrangement of Allylic Esters. *ChemistrySelect* **2020**, *5*, 2559-2563; (f) Huang, Q.-A.; Haruta, A.; Kumamoto, Y.; Murayama, H.; Yamamoto, E.; Honma, T.; Okumura, M.; Nobutou, H.; Tokunaga, M., Pt/CeO₂ with residual chloride as reusable soft Lewis acid catalysts: Application to highly efficient isomerization of allylic esters. *Applied Catalysis B: Environmental* **2021**, *296*, 120333; (g) Liu, Y.; Liu, X.; Feng, X., Recent advances in metal-catalysed asymmetric sigmatropic rearrangements. *Chem. Sci.* **2022**, *13*, 12290-12308; (h) Lee, H.; Kim, K. T.; Kim, M.; Kim, C., Recent advances in catalytic [3, 3]-sigmatropic rearrangements. *Catalysts* **2022**, *12*, 227.

4. (a) Cahiez, G.; Moyeux, A., Cobalt-catalyzed cross-coupling reactions. *Chem. Rev.* **2010**, *110*, 1435-1462; (b) Pellissier, H.; Clavier, H., Enantioselective cobalt-catalyzed transformations. *Chem. Rev.* **2014**, *114*, 2775-2823; (c) Gandeepan, P.; Cheng, C.-H., Cobalt catalysis involving π components in organic synthesis. *Acc. Chem. Res.* **2015**, *48*, 1194-1206; (d) Ai, W.; Zhong, R.; Liu, X.; Liu, Q., Hydride transfer reactions catalyzed by cobalt complexes. *Chem. Rev.* **2018**, *119*, 2876-2953; (e) Susan Treesa, G.; Neetha, M.; Saranya, S.; Anilkumar, G., Cobalt‐Catalyzed Multi‐Component Reactions: Recent Advances and Perspectives in Organic Synthesis. *ChemistrySelect* **2020**, *5*, 7400-7416; (f) Michiyuki, T.; Komeyama, K., Recent advances in four‐coordinated planar cobalt catalysis in organic synthesis. *Asian J. Org. Chem.* **2020**, *9*, 343-358; (g) Lukasevics, L.; Grigorjeva, L., Cobalt-catalyzed carbonylation of the C–H bond. *Organic & Biomolecular Chemistry* **2020**, *18*, 7460-7466; (h) Han, J.-F.; Guo, P.; Zhang, X.-G.; Liao, J.-B.; Ye, K.-Y., Recent advances in cobalt-catalyzed allylic functionalization. *Organic & Biomolecular Chemistry* **2020**, *18*, 7740-7750; (i) Lukasevics, L.; Cizikovs, A.; Grigorjeva, L., C–H bond functionalization by high-valent cobalt catalysis: current progress, challenges and future perspectives. *Chem. Commun.* **2021**, *57*, 10827-10841; (j) Yang, X.; Ge, S., Recent progress in cobalt-catalyzed enantioselective hydrogenation and hydroboration reactions of alkenes. *Current Opinion in Green and Sustainable Chemistry* **2021**, *31*, 100542; (k) Tohidi, M. M.; Paymard, B.; Vasquez-García, S. R.; Fernández-Quiroz, D., Recent progress in applications of cobalt catalysts in organic reactions. *Tetrahedron* **2023**, *136*, 133352; (l) Jose, J.; Mathew, T. V., Cobalt‐Catalyzed Hydrosilylation across Carbon‐Carbon, Carbon‐Oxygen, and Carbon‐Nitrogen Multiple Bonds – A Comprehensive Review. *ChemCatChem* **2024**, e202301626.

5. (a) Schmidt, A.; Nödling, A. R.; Hilt, G., An Alternative Mechanism for the Cobalt‐Catalyzed Isomerization of Terminal Alkenes to (Z)‐2‐Alkenes. *Angew. Chem. Int. Ed.* **2015**, *54*, 801-804; (b) Crossley, S. W.; Barabé, F.; Shenvi, R. A., Simple, chemoselective, catalytic olefin isomerization. *J. Am. Chem. Soc.* **2014**, *136*, 16788-16791; (c) Crossley, S. W.; Obradors, C.; Martinez, R. M.; Shenvi, R. A., Mn-, Fe-, and Co-catalyzed radical hydrofunctionalizations of olefins. *Chem. Rev.* **2016**, *116*, 8912-9000; (d) Green, S. A.; Crossley, S. W.; Matos, J. L.; Vásquez-Céspedes, S.; Shevick, S. L.; Shenvi, R. A., The high chemofidelity of metal-catalyzed hydrogen atom transfer. *Acc. Chem. Res.* **2018**, *51*, 2628-2640; (e) Liu, X.; Zhang, W.; Wang, Y.; Zhang, Z.-X.; Jiao, L.; Liu, Q., Cobalt-catalyzed regioselective olefin isomerization under kinetic control. *J. Am. Chem. Soc.* **2018**, *140*, 6873-6882; (f) Meng, Q. Y.; Schirmer, T. E.; Katou, K.; König, B., Controllable isomerization of alkenes by dual visible‐light‐cobalt catalysis. *Angew. Chem. Int. Ed.* **2019**, *58*, 5723-5728; (g) Zhao, J.; Cheng, B.;

Chen, C.; Lu, Z., Cobalt-catalyzed migrational isomerization of styrenes. *Org. Lett.* **2020**, *22*, 837-841; (h) Zhang, S.; Bedi, D.; Cheng, L.; Unruh, D. K.; Li, G.; Findlater, M., Cobalt (II)-catalyzed stereoselective olefin isomerization: facile access to acyclic trisubstituted alkenes. *J. Am. Chem. Soc.* **2020**, *142*, 8910-8917; (i) Shen, X.; Chen, X.; Chen, J.; Sun, Y.; Cheng, Z.; Lu, Z., Ligand-promoted cobalt-catalyzed radical hydroamination of alkenes. *Nat. Commun.* **2020**, *11*, 783; (j) Kim, D.; Pillon, G.; DiPrimio, D. J.; Holland, P. L., Highly Z-selective double bond transposition in simple alkenes and allylarenes through a spin-accelerated allyl mechanism. *J. Am. Chem. Soc.* **2021**, *143*, 3070-3074; (k) Liu, W.; Zheng, Y.; Mao, Y.; Chen, J.; Ren, X.; Cheng, Z.; Lu, Z., Desymmetrizing isomerization of alkene via thiazolinyl iminoquinoline cobalt catalysis. *Org. Lett.* **2022**, *24*, 1158-1163; (l) Herbort, J. H.; Bednar, T. N.; Chen, A. D.; RajanBabu, T.; Nagib, D. A., γ C–H functionalization of amines via triple H-atom transfer of a vinyl sulfonyl radical chaperone. *J. Am. Chem. Soc.* **2022**, *144*, 13366-13373; (m) Rong, X.; Yang, J.; Liu, S.; Lan, Y.; Liu, Q., Remote Stereocontrol of All-Carbon Quaternary Centers via Cobalt-Catalyzed Asymmetric Olefin Isomerization. *CCS Chemistry* **2023**, *5*, 1293-1300.

6. (a) Occhialini, G.; Palani, V.; Wendlandt, A. E., Catalytic, contra-thermodynamic positional alkene isomerization. *J. Am. Chem. Soc.* **2021**, *144*, 145-152; (b) Palani, V.; Wendlandt, A. E., Strain-Inducing Positional Alkene Isomerization. *J. Am. Chem. Soc.* **2023**, *145*, 20053-20061.

7. (a) Surzur, J.; Teissier, P., Addition Radicalaire Desters Sur Les Alcools Ethyleniques. *C. R. Acad. Sci. Fr. Ser. C* **1967**, *264*, 1981-1984; (b) Tanner, D. D.; Law, F. C., Free-radical acetoxy group migration. *J. Am. Chem. Soc.* **1969**, *91*, 7535-7537; (c) Beckwith, A. L. J.; Crich, D.; Duggan, P. J.; Yao, Q., Chemistry of β-(Acyloxy)alkyl and β-(Phosphatoxy)alkyl Radicals and Related Species: Radical and Radical Ionic Migrations and Fragmentations of Carbon–Oxygen Bonds. *Chem. Rev.* **1997**, *97*, 3273-3312.

8. Obradors, C.; Martinez, R. M.; Shenvi, R. A., Ph (i-PrO) SiH₂: an exceptional reductant for metal-catalyzed hydrogen atom transfers. *J. Am. Chem. Soc.* **2016**, *138*, 4962-4971.

9. (a) Cernak, T.; Dykstra, K. D.; Tyagarajan, S.; Vachal, P.; Krska, S. W., The medicinal chemist's toolbox for late stage functionalization of drug-like molecules. *Chem. Soc. Rev.* **2016**, *45*, 546-576; (b) Moir, M.; Danon, J. J.; Reekie, T. A.; Kassiou, M., An overview of late-stage functionalization in today's drug discovery. *Expert Opin. Drug Discov.* **2019**, *14*, 1137-1149; (c) Börgel, J.; Ritter, T., Late-stage functionalization. *Chem* **2020**, *6*, 1877-1887; (d) Guillemard, L.; Kaplaneris, N.; Ackermann, L.; Johansson, M. J., Late-stage C–H functionalization offers new opportunities in drug discovery. *Nat. Rev. Chem.* **2021**, *5*, 522-545; (e) Jana, R.; Begam, H. M.; Dinda, E., The emergence of the C–H functionalization strategy in medicinal chemistry and drug discovery. *Chem. Commun.* **2021**, *57*, 10842-10866; (f) Nippa, D. F.; Hohler, R.; Stepan, A. F.; Grether, U.; Konrad, D. B.; Martin, R. E., Late-stage functionalization and its impact on modern drug discovery: Medicinal chemistry and chemical biology highlights. *Chimia* **2022**, *76*, 258-258; (g) Castellino, N. J.; Montgomery, A. P.; Danon, J. J.; Kassiou, M., Late-stage Functionalization for Improving Drug-like Molecular Properties. *Chem. Rev.* **2023**, *123*, 8127-8153.

10. Zhao, G.; Kaur, S.; Wang, T., Visible-light-mediated thiol–ene reactions through organic photoredox catalysis. *Org. Lett.* **2017**, *19*, 3291-3294.

11. Legault, C. Y., *CYLview20*, Université de Sherbrooke, **2020** http://www.cylview.org.

12. Zhao, G.; Lim, S.; Musaev, D. G.; Ngai, M.-Y., Expanding reaction profile of allyl carboxylates via 1, 2-radical migration (RaM): visible-light-induced phosphine-catalyzed 1, 3-carbobromination of allyl carboxylates. *J. Am. Chem. Soc.* **2023**, *145*, 8275-8284.

Insert Table of Contents artwork here

allyl
carboxylate

1,2-Radical Migration (RaM)

I

II

1,3-alkene &
1,2-acyloxy shift

- new reaction profile of allyl carboxylates ■ atom-economic and redox-neutral reaction
- unprecedented 1,3-alkene/1,2-acyloxy shift product formation ■ gram-scale synthesis
- homolytic activation of C-O bonds of allyl carboxylates ■ late-stage functionalization